

# An essential role for stromal interaction molecule 1 in neointima formation following arterial injury

Rui-Wei Guo<sup>1†</sup>, Hong Wang<sup>1†</sup>, Pan Gao<sup>1</sup>, Mao-Quan Li<sup>2</sup>, Chun-Yu Zeng<sup>3</sup>, Yang Yu<sup>1</sup>, Jian-Fei Chen<sup>1</sup>, Ming-Bao Song<sup>1</sup>, Yan-Kun Shi<sup>1</sup>, and Lan Huang<sup>1\*</sup>

<sup>1</sup>Department of Cardiology, Xinqiao Hospital, Third Military Medical University, Chongqing 400037, China; <sup>2</sup>Department of Public Health, Chengdu Medical College, Chengdu 610000, China; and <sup>3</sup>Department of Cardiology, Daping Hospital, Third Military Medical University, Chongqing 400037, China

Received 18 July 2008; revised 28 November 2008; accepted 1 December 2008; online publish-ahead-of-print 3 December 2008

Time for primary review: 27 days

## KEYWORDS

STIM1;  
VSMC proliferation;  
Neointimal;  
Vascular injury;  
Restenosis

**Aims** There is evidence to suggest that stromal interaction molecule 1 (STIM1) functions as a Ca<sup>2+</sup> sensor on the endoplasmic reticulum, leading to transduction of signals to the plasma membrane and opening of store-operated Ca<sup>2+</sup> channels (SOC). SOC have been detected in vascular smooth muscle cells (VSMCs) and are thought to have an essential role in the regulation of contraction and cell proliferation. We hypothesized that knockdown of STIM1 inhibits VSMC proliferation and suppresses neointimal hyperplasia.

**Methods and results** We examined the effect of the knockdown of STIM1 using a rat balloon injury model and cultured rat aortic VSMCs. Interestingly, knockdown of rat STIM1 by adenovirus delivery of small interfering RNA (siRNA) significantly suppressed neointimal hyperplasia in a rat carotid artery balloon injury model at 14 days after injury. The re-expression of human STIM1 to smooth muscle reversed the effect of STIM1 knockdown on neointimal formation. Rat aortic VSMCs were used for the *in vitro* assays. Knockdown of endogenous STIM1 significantly inhibited proliferation and migration of VSMCs. Moreover, STIM1 knockdown induced cell-cycle arrest in G0/G1 and resulted in a marked decrease in SOC. Replenishment with recombinant human STIM1 reversed the effect of siRNA knockdown. These results suggest STIM1 has a critical role in neointimal formation in a rat model of vascular injury.

**Conclusion** STIM1 may represent a novel therapeutic target in the prevention of restenosis after vascular interventions.

## 1. Introduction

The atherosclerotic process is characterized by the recruitment of monocytes and lymphocytes to the arterial intima. The subsequent accumulation and proliferation of vascular smooth muscle cells (VSMCs), which immigrate from the medial layer, lead to lesion progression and encroachment on the coronary vascular lumen.<sup>1</sup> Despite the fact that the use of percutaneous coronary intervention (PCI) has improved the results of atherosclerosis significantly, understanding restenosis after PCI remains a challenge. Restenosis refers to the re-occurrence of stenosis on the basis of intimal lesion, and the major contribution to this process is the proliferation and migration of medial VSMCs.<sup>2</sup> Therefore, proliferation of VSMCs is a key event in atherosclerosis and restenosis after vascular injury; however, the underlying mechanism of VSMCs' proliferation is unclear.

Ca<sup>2+</sup> channels are of particular interest in cell proliferation because of the profound anti-proliferative effect of

removing extracellular Ca<sup>2+</sup> and evidence from studies of many cell types that Ca<sup>2+</sup> entry mechanisms have an essential role.<sup>3,4</sup> Elevation of Ca<sup>2+</sup> levels in VSMCs can result from entry of extracellular Ca<sup>2+</sup> as well as release of Ca<sup>2+</sup> sequestered within organelles such as the sarcoplasmic reticulum (SR). Ca<sup>2+</sup> influx across the plasma membrane (PM) is mediated by voltage-dependent Ca<sup>2+</sup> channels, and voltage-independent cation channels, including store-operated Ca<sup>2+</sup> channels (SOC).<sup>5,6</sup> It has been recognized that phenotypic modulation of VSMCs is associated with downregulation of voltage-dependent Ca<sup>2+</sup> channels, which provide Ca<sup>2+</sup> entry for contraction when the cells are in the contractile phenotype of the physiological blood vessel and are the target of antihypertensive calcium antagonist drugs.<sup>6</sup> What are the Ca<sup>2+</sup> channels of the proliferating VSMCs? Store-operated Ca<sup>2+</sup> entry (SOCE), also known as capacitative Ca<sup>2+</sup> entry, is thought to have an essential role in the regulation of contraction, cell proliferation, and apoptosis.<sup>7–9</sup> Meanwhile, it has been reported that SOCE has been detected in VSMCs.<sup>10</sup>

The activation of SOCE is triggered by a reduction in the concentration of SR Ca<sup>2+</sup>. Transient discharge of SR Ca<sup>2+</sup>

\* Corresponding author. Tel: +86 23 68755601; fax: +86 23 68755601.  
E-mail address: huanglan260@126.com

† R.W.G. and H.W. contributed equally to this work.

occurs during the course of signalling events that activate inositol 1,4,5-trisphosphate receptors or ryanodine receptors in the SR membrane. SR  $\text{Ca}^{2+}$  stores can be depleted by inhibiting sarcoendoplasmic reticulum  $\text{Ca}^{2+}$  ATPases with thapsigargin (TG).<sup>11</sup> Although several biophysically distinct SOCE have been reported, the best characterized are the  $\text{Ca}^{2+}$  release-activated  $\text{Ca}^{2+}$  (CRAC) channels. Over the years, many genes have been claimed to code for the CRAC channel. Recently, an RNAi-based screening approach revealed a novel membrane-spanning protein named stromal interaction molecule 1 (STIM1) to be required for the activation of SOCE.<sup>12</sup> STIM1 is dispersed on the endoplasmic reticulum (ER) membrane under quiescence.  $\text{Ca}^{2+}$  store depletion stimulates redistribution of STIM1 to the PM. The redistribution is thought to transmit a store depletion signal to the CRAC channels in the PM. Evidence indicates that STIM1 may function as a  $\text{Ca}^{2+}$  sensor in the ER, leading to transduction of this signal to the PM and opening of SOC located in the PM.<sup>12,13</sup> Nevertheless, there has been relatively little association of STIM1 with human disease, little direct evidence that STIM1 knockdown could be an effective therapeutic strategy, and no link between STIM1 and organ function. We have focused on the suggestion that STIM1 might have a role in vascular disease. Here, we present evidence from *in vivo* and *in vitro* studies that STIM1 does have an essential role in the proliferation of VSMCs, and we consider the relevance to the adaptive injury response of blood vessels.

## 2. Methods

### 2.1 Reagents

The one-step RT-PCR kit was from TaKaRa (Shiga, Japan). The anti-STIM1 antibody (25–139) was purchased from BD (NJ, USA); anti-PCNA were from Santa Cruz (CA, USA); and anti-smooth muscle  $\alpha$ -actin (SM $\alpha$ A) antibody were from NeoMarkers (CA, USA); anti-pRb, anti-p21, and anti- $\beta$ -actin antibody were from Sigma (MO, USA). Fetal bovine serum (FBS) was obtained from HyClone (UT, USA). Medium and supplements were purchased from Gibco BRL (NY, USA). Fura-2AM was obtained from Beyotime Chemical Company (Jiangsu, China). TG was from Sigma (MO, USA).

### 2.2 Construction of adenoviral vectors

All small interfering RNA (siRNA) sequences were designed as described.<sup>14</sup> A mixture of two siRNA duplex sequences exclusively targeting rat STIM1 (rSTIM1, GenBank accession number NM\_001108496), but not human STIM1 (hSTIM1, GenBank accession number U52426) were used. (i) Start nucleotide 935, GCAUGGAAGGCAUCAGAAGUGUAUA; and (ii) start nucleotide 970, GGAUGAGGUGAUACAGUGGCUGAUU. A non-silencing control (NSC) sequence was designed according to the sequence of a negative control. Target sequences for rSTIM1 were chemically synthesized (Genesil, China) as complementary oligonucleotides. Annealed oligonucleotides encoding sense and antisense strands linked by the loop sequence were subcloned into pGS-1 (Genesil, China). hSTIM1 DNA expression constructs were as described.<sup>14</sup> The 2.7 kb fragment of hSTIM1 was subcloned into pGS-1 either as a wild-type cDNA fragment or after introduction of a premature stop codon (PEST), producing a 597 amino acid residue PEST protein without the two proline-rich regions (residues 617–634 and 651–671). Recombinant viral genomes were transfected into 293 cells in a 6-well plate using METAFECTENE<sup>TM</sup> (Biontexas). Eight days after transfection, the recombinant virus was collected and subjected to one round of amplification in a T-75 flask with  $1.5 \times 10^6$  293 cells, resulting in

2 mL of viral stock. The Ad-si/rSTIM1 and Ad-hSTIM1 viruses were titrated using the standard plaque assay. The titre for Ad-si/STIM1 was  $3 \times 10^9$  plaque-forming units (pfu)/mL. All adenoviruses expressed GFP under a separate promoter, allowing verification of infection. An NSC sequence was generated in the same manner.

### 2.3 Balloon angioplasty and delivery of adenoviruses

Male Wistar rats weighing 250–300 g (Chongqing, China) were anaesthetized with an intramuscular injection of 100 mg/kg ketamine and 5 mg/kg xylazine. Angioplasty of the left carotid artery was performed by using a balloon embolectomy catheter (1.5F, Cordis; USA) as described.<sup>15</sup> The balloon catheter was introduced through the left external carotid artery into the common carotid artery and inflated at 2 atm with a calibrated inflation device. The carotid artery was damaged by passing the inflated balloon catheter back and forth through the lumen three times. Some animals were subjected to anaesthesia and surgical procedure without balloon injury (sham-operated rats). After balloon injury, solutions of (20  $\mu$ L) Ad-si/rSTIM1 ( $3 \times 10^9$  pfu/mL), Ad-hSTIM1 ( $3 \times 10^9$  pfu/mL), or NSC ( $3 \times 10^9$  pfu/mL) were infused into the ligated segment of the common carotid artery for 20 min. The ligatures and catheter were then removed, the external carotid artery was ligated, and the incision was closed. At 7 days and 14 days after arteriotomy, rats were anaesthetized and carotid arteries were carefully dissected free from surrounding tissue and perfused at physiological pressure with 4% paraformaldehyde in PBS for fixation. The balloon injury model used is purely one of proliferation. All studies conformed to the Guide for the Care and Use of Laboratory Animals published by the US National Institutes of Health (NIH Publication no. 85-23, revised 1996).

### 2.4 Cell culture and adenoviral transduction

Rat aortic VSMCs were isolated and subcultured as described.<sup>16</sup> VSMCs between three and seven passages were quiesced by incubating in serum-free DMEM for 24 h at 37°C and used for the *in vitro* experiments unless stated otherwise. VSMCs were transduced with Ad-si/rSTIM1, Ad-hSTIM1, or NSC, and STIM1 protein levels were evaluated in the cell extracts.

### 2.5 Morphology

Morphometry was performed as described.<sup>17</sup> Briefly, at 7 and 14 days after angioplasty, animals were anaesthetized as described above, and the carotid arteries were fixed by perfusion with 100 mL of PBS (pH 7.2), followed by 80 mL of PBS containing 4% paraformaldehyde through a large cannula placed in the left ventricle. The carotid arteries were removed, and six cross-sections were cut from the approximate middle of the artery. The sections were stained with haematoxylin and eosin to demarcate cell types and were photographed under low power, video-digitized, and stored in an image analysis system. The media, neointima, and vessel walls were traced carefully, and the neointima and media area was calculated. To investigate the lumen loss of each group, the lumen area of injured carotid (LAI) was measured and normalized by the arterial area measure of the contralateral non-injured carotid (LAC) of the same animal. The lumen loss ratio was calculated as: lumen loss ratio =  $(\text{Lac} - \text{LAI})/\text{Lac} \times 100\%$ .

### 2.6 Western blotting

The injured vessels without adventitia or VSMC protein were extracted as described.<sup>16</sup> Equal amounts of protein were separated by SDS-PAGE (10% polyacrylamide gel). The protein was subsequently transferred onto a polyvinylidene difluoride membrane by electroblotting for 3 h at 150 mA. The membrane was blocked in a 5% non-fat milk solution in TBS with 0.5% Tween 20. The membrane was allowed to react with primary antibody and detection of

specific proteins was done by enhanced chemiluminescence following the manufacturer's instructions. Densitometric signals were quantified by Quantity One.

## 2.7 Transwell migration assay

The effect of STIM1 knockdown on VSMCs migration was determined by a transwell migration assay as described.<sup>18</sup> Briefly, VSMCs were transfected with adenovirus expressing NSC, siRNAs against rSTIM1, and siRNAs against rSTIM1 plus hSTIM1. At 48 h after transfection, VSMCs (25 000 cells/chamber) were plated onto the upper chamber of Transwell (Costar) inserts with 8  $\mu\text{m}$  pore size (BD-Biosciences). Chemotaxis was achieved by the presence of 5% serum in the chamber bottom. After 4 h, the transwell chambers were rinsed in PBS, and cells on top of the chamber were removed with a cotton swab. Cells on the bottom of the Transwell membrane were fixed with 4% paraformaldehyde at 37°C for 15 min, and then rinsed with PBS. To quantify the number of migrating cells on the bottom of the Transwell, cells were labelled with DAPI, and then cells that had migrated were counted manually using a fluorescent microscope. In all cases, five separate high-power fields were counted per membrane.

## 2.8 RNA isolation and real-time RT-PCR

Total RNA was isolated with TRIzol<sup>®</sup> reagent according to the manufacturer's protocol.<sup>19</sup> Total RNA was reverse-transcribed into cDNA, and the resultant cDNA was amplified by SYBR Green1 fluorescence real-time RT-PCR. The PCR reaction was directly monitored by the Bioer FQD-66A sequence detection system. The primers for rSTIM1 were 5'-ATTTGACCCATTCCGATTC-3' (forward) and 5'-GGCTATGAGAA TGGGAAGA-3' (reverse). The primers for  $\beta$ -actin were 5'-CACCCG CGAGTACAACCTTC-3' (forward) and 5'-CCCATACCCACCACACACC-3' (reverse). The single-stranded cDNA was amplified by PCR using 35 cycles. The PCR profile used for rSTIM1 amplification was: 30 s of denaturation at 94°C, 30 s of annealing at 59°C, and 1.5 min of extension at 72°C. The profile for  $\beta$ -actin amplification was: 30 s of denaturation at 94°C, 30 s of annealing at 57°C, and 1.5 min of extension at 72°C. The results were expressed as mean  $\pm$  SD for the relative expression levels.

## 2.9 Cell-cycle analysis and cell counting

Cell-cycle distribution was analysed using flow cytometry. Briefly, VSMCs were trypsinized, washed with PBS, and fixed in 80% ethanol. They were then washed with PBS, incubated with 100 mg/mL RNase at 37°C for 30 min, stained with propidium iodide (50 mg/mL), and analysed on a FACScan flow cytometer. The percentage of cells in different phases of the cell cycle was determined using the Cell-FIT software. The growth curves of VSMCs were examined using cell counting. Cells first underwent mitogenic quiescence by serum starvation and viral infection. The cell number under these experimental conditions was used as the baseline. To examine the status of VSMC proliferation, the cells were subsequently stimulated with serum (10% FBS), and the cell number was counted every day for 3 days. Each count was an average of three repeats, and each datum point was the average of three experiments.

## 2.10 Double-immunofluorescence staining

Carotid arteries were snap-frozen in liquid nitrogen in OCT embedding medium and stored at  $-80^{\circ}\text{C}$ . Six cross-sections were cut (6  $\mu\text{m}$ ) from the approximate middle portion of the artery and used for STIM1 and SM $\alpha$ A detection by immunofluorescence.<sup>20</sup> For staining, sections were fixed in acetone for 10 min, air dried, and rehydrated with PBS before incubation in serum-free protein block for 30 min. To detect STIM1, sections were stained with anti-rat STIM1 antibody (mouse IgG) diluted in 1% blocking reagent/0.3% Triton X-100 in PBS overnight before being washed in TNT wash

buffer (Tris-HCl, pH 7.5, 0.15 mol/L NaCl, and 0.05% Tween 20, Sigma). Sections incubated with an isotype-matched control antibody were used as negative control. Subsequently, sections were incubated with TRITC-goat anti-mouse IgG for 30 min before washing. Anti-rat SM $\alpha$ A (rabbit IgG) and FITC-goat anti-rabbit IgG were used for detecting SM $\alpha$ A as described above. Images were taken by a confocal laser scanning microscope (Leica TCS SP5, Germany).

## 2.11 Measurement of intracellular free $\text{Ca}^{2+}$ , $[\text{Ca}^{2+}]_i$

The VSMCs were loaded with the calcium indicator Fura-2AM (5  $\mu\text{M}$ ) in Hepes-buffered saline. Changes in  $[\text{Ca}^{2+}]_i$  in individual cells were measured using an Aquacosmos system with band-pass filters for 340 and 380 nm.  $[\text{Ca}^{2+}]_i$  was calculated from the Fura-2 fluorescence ratio (F340/F380) using linear regression between adjacent points on a calibration curve generated by measuring F340/F380 in at least seven calibration solutions containing  $\text{Ca}^{2+}$  at concentrations between 0 and 854 nM. The SOC-mediated influx of  $\text{Ca}^{2+}$  following stimulation with 1  $\mu\text{M}$  TG during the change from  $\text{Ca}^{2+}$ -free conditions to 2 mM  $\text{Ca}^{2+}$  was measured as described.<sup>21</sup>

## 2.12 [<sup>3</sup>H]Thymidine incorporation

VSMC DNA synthesis was measured by [<sup>3</sup>H]thymidine incorporation as described.<sup>22</sup> Confluent VSMCs in 100 mm dishes were detached with 0.05% trypsin/EDTA, seeded onto 24-well plates (10,000 cells/well) in 10% FBS/DMEM, and allowed to attach overnight. VSMCs were starved in serum-free DMEM for 24 h and then incubated for 48 h with adenoviral vectors as indicated. During the final 4 h of the assay, 1  $\mu\text{Ci}$  of [methyl-<sup>3</sup>H]-thymidine was added to each well. Incorporated <sup>3</sup>H-thymidine was precipitated with 10% trichloroacetic acid and counted with a liquid scintillation counter.

## 2.13 Statistical analysis

Results are expressed as mean  $\pm$  SEM of *n* rats for *in vivo* experiments and mean  $\pm$  SEM of multiple experiments for molecular biology. SPSS13.0 software was used for statistical analysis. Student's *t*-tests were used to compare the two groups, or ANOVA was used with Tukey's multiple comparison tests for multiple groups. Values of *P* < 0.05 were regarded as statistically significant.

## 3. Results

### 3.1 Expression of STIM1 in rat carotid arteries after balloon angioplasty

To determine whether STIM1 mRNA and protein were expressed in rat carotid arteries after balloon angioplasty, real-time RT-PCR and western blotting were done with total RNA and cytosolic protein extracts from carotid arteries. STIM1 mRNA and protein were detected in carotid arteries subjected to vascular injury, whereas their expression was low in uninjured right carotid arteries at 7 and 14 days after balloon angioplasty (Figure 1A and B). Meanwhile, when compared with the sham groups, STIM1 mRNA and protein in the left injured carotid had increased significantly at 7 days after balloon angioplasty and further increased at 14 days after balloon angioplasty. We conclude from these observations that the expression of STIM1 was upregulated after balloon angioplasty.

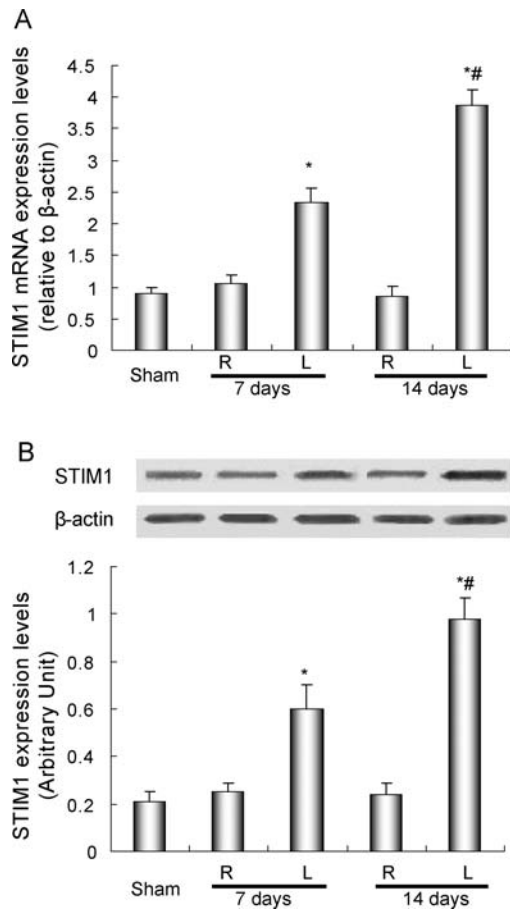


**Figure 1** (A) Time-course analysis of stromal interaction molecule 1 mRNA expression in carotid arteries after balloon angioplasty. Parallel amplification of the rat housekeeping  $\beta$ -actin gene was used as an internal control. The results are expressed as mean  $\pm$  SEM of six experiments. \* $P < 0.05$  vs. sham groups or R at days 7 and 14; # $P < 0.05$  vs. L at day 7 after balloon angioplasty. (B) Top: Western blot analysis was used for cytosolic extracts of pooled carotid arteries at different time points after balloon angioplasty. Equal loading was confirmed by staining  $\beta$ -actin. The data shown are representative of six different experiments. Bottom: Densitometric analysis of stromal interaction molecule 1 protein expression levels, normalized to expression levels of the housekeeping  $\beta$ -actin gene, was determined by Quantity One program. The results are expressed as mean  $\pm$  SEM of six experiments. \* $P < 0.05$  vs. sham groups or R; # $P < 0.05$  vs. L at 7 days after balloon. R, uninjured right carotid arteries; L, injured left carotid arteries; sham, sham-operated rats at 0 day.

### 3.2 Localization of STIM1 and SM $\alpha$ A in rat carotid arteries

Localization of STIM1 and SM $\alpha$ A-positive cells in rat carotid arteries was done by double-immunofluorescence staining to determine the spatial distribution and cellular localization of STIM1. A clear immunoreactivity for STIM1 and SM $\alpha$ A was detected in the media at 7 days and 14 days after balloon angioplasty (Figure 2). In addition, immunoreactivity for STIM1 and SM $\alpha$ A was observed mostly in neointima at days 7 and 14. These results suggest that STIM1 is expressed in proliferating SMCs, contributing greatly to neointimal formation.

### 3.3 STIM1 silencing attenuates neointima formation *in vivo*

We first examined the efficiency of adenovirus transfection in rat carotid arteries by western blot analysis. The level of GFP expression reached a maximum at day 3 and

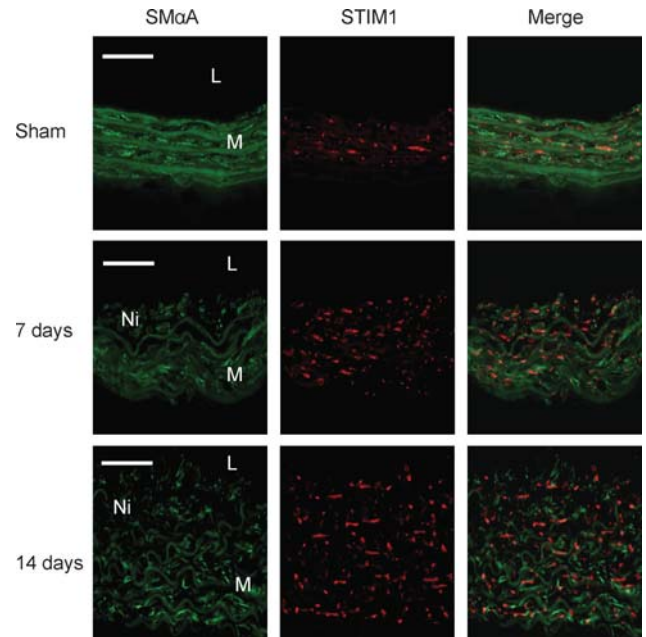


**Figure 2** Double-immunofluorescence staining of SM $\alpha$ A (green) and stromal interaction molecule 1 (red) in rat carotid arteries 7 and 14 days after balloon angioplasty. The results illustrated are from a single experiment and are representative of three separate experiments. L, lumen; M, media; Ni, neointima; sham: sham-operated rats at 0 day. All bars represent 50  $\mu$ m.

remained high until days 7 and 14 after adenoviral infection. These results suggest that the adenovirus-mediated delivery system was effective in rat carotid artery (see Supplementary material online, Figure S1). We delivered adenovirus constructs expressing NSC, Ad-hSTIM1, and Ad-si/rSTIM1 to rat carotid arteries. Expression of STIM1 protein (without adventitia) was confirmed by western blotting. Compared with the NSC group, incubation with Ad-si/rSTIM1 attenuated injury-induced STIM1 upregulation significantly. Cotransfection with Ad-hSTIM1 reversed the downregulation of STIM1 by RNAi (Figure 3A). Interestingly, the neointimal formation area and lumen loss ratio at day 14 were reduced significantly by transfection with Ad-si/rSTIM1 compared with transfection with NSC. When Ad-hSTIM1 was transfected with Ad-si/rSTIM1, the neointimal formation area and lumen loss ratio were restored to near the control level (Figure 3B and C, Supplementary material online, Figure S2). These results indicated that inhibition of STIM1 could reduce neointimal hyperplasia *in vivo*. Concomitantly, the expression of PCNA in rat carotid arteries at 14 days after injury was much lower in the Ad-si/rSTIM1-treated group than in the NSC group. The transfection of Ad-hSTIM1 with Ad-si/rSTIM1 restored the expression of PCNA in rat carotid arteries to near the level of that in the NSC group. In addition, STIM1 knockdown caused an increase in the expression of p21, and a significant reduction in the phosphorylation of Rb (pRb) *in vivo* at 14 days after injury. No significant differences were found between the sham group and the Ad-si/rSTIM1-treated group on the expression of PCNA, p21, and pRb (Figure 3D).

### 3.4 Suppression of STIM1 inhibits VSMCs proliferation and migration *in vitro*

The VSMCs are the primary cell type transduced by adenovirus in the rat balloon injury model and the major cell

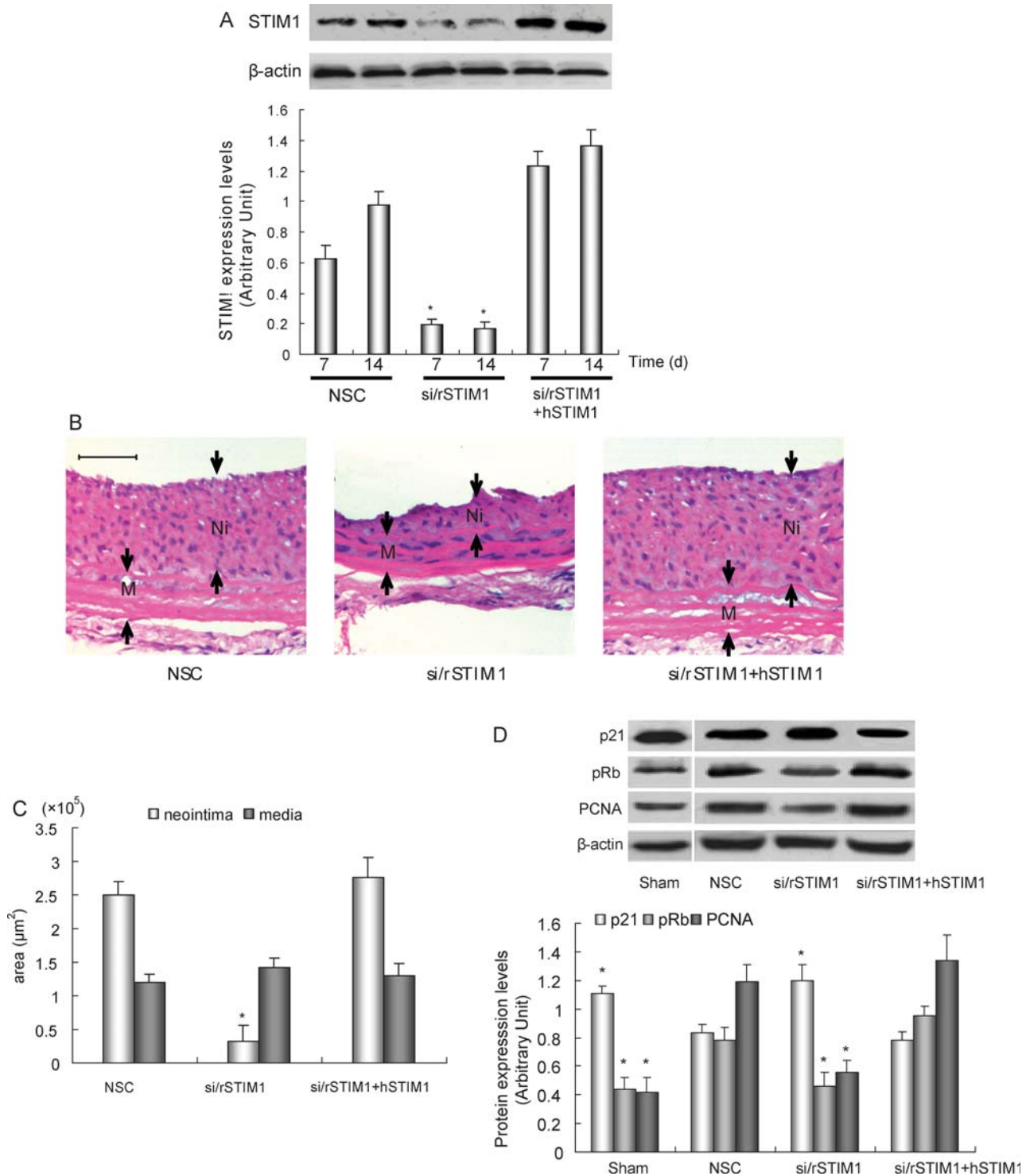


**Figure 3** (A) Top: Western blot for stromal interaction molecule 1 and  $\beta$ -actin of rat carotid arteries (whole artery) at 7 and 14 days after balloon injury and gene delivery. The data shown are representative of six different experiments. Bottom: Densitometric analysis of stromal interaction molecule 1 protein expression levels, normalized to expression levels of the housekeeping  $\beta$ -actin gene, was determined by Quantity One program. The results are expressed as mean  $\pm$  SEM of six experiments. \* $P < 0.05$  vs. NSC (non-silencing control) and small interfering RNAs against rSTIM1 plus hSTIM1. (B) Cryosections of carotid artery at 14 days after balloon injury and gene delivery were stained with haematoxylin and eosin. M, media; Ni, neointima. The bar represents 50  $\mu$ m. (C) Intimal and media area was compared among rat carotid arteries transfected with adenovirus expressing non-silencing control, small interfering RNAs against rSTIM1, and small interfering RNAs against rSTIM1 plus hSTIM1. The results are expressed as mean  $\pm$  SEM of six experiments. \* $P < 0.05$  vs. intima area at non-silencing control and small interfering RNAs against the rSTIM1 plus hSTIM1 group. (D) Western blot for p21, pRb, PCNA, and  $\beta$ -actin of rat carotid arteries at 14 days after balloon injury and gene delivery. Sham-operated rats at 0 day served as controls. The data shown are representative of three different experiments. Data are presented as the mean  $\pm$  SEM ( $n = 3$ ). \* $P < 0.05$  vs. non-silencing control and si/rSTIM1+hSTIM1. sham, sham-operated rats at 0 day.

type contributing to neointimal hyperplasia after balloon injury. To determine whether endogenous STIM1 had an effect on VSMC proliferation, rat aortic VSMCs were cultured

for use in *in vitro* experiments. Adenovirus constructs expressing NSC, hSTIM1, and si/rSTIM1 were added to rat aortic VSMCs. The transfection efficiency of adenovirus

GFP expression in cultured VSMCs was  $92.4 \pm 7.6\%$  (see Supplementary material online, *Figure S3*). The basal and induced STIM1 levels were detected *in vitro* by immunoblotting. In addition, the effects of STIM1 silencing in non-stimulated and stimulated VSMCs also were demonstrated at 48 h post-transduction (see Supplementary material online, *Figure S4*). Transduction of VSMCs with Ad-si/rSTIM1 (MOI 15 and 30 pfu/cell) effectively decreased STIM1 protein expression at 48 h post-transduction. The cotransfection of Ad-hSTIM1 (MOI 15 pfu/cell) with Ad-si/rSTIM1 (MOI 15 pfu/cell) restored the expression of STIM1 protein (*Figure 4A*). Interestingly, transfection of VSMCs with Ad-si/rSTIM1 decreased the uptake of [ $^3$ H]thymidine by VSMCs significantly at 48 h after infection. The cotransfection of Ad-hSTIM1 reversed the effect of STIM1 knockdown on [ $^3$ H]thymidine uptake (*Figure 4B*). Concomitantly, transfection of VSMCs with Ad-si/rSTIM1 suppressed proliferation of VSMCs significantly (MOI 15 pfu/cell), and hSTIM1 re-expression reversed the effect of STIM1 knockdown on VSMC proliferation (*Figure 4C*). These results demonstrated that knockdown of STIM1 could suppress VSMC proliferation *in vitro*.

Transwell assays were used to assess the effects of STIM1 knockdown on migrated cells. Transfection of VSMCs with Ad-si/rSTIM1 decreased the number of migrating cells significantly at 48 h after infection. In this rSTIM1 knockdown background, hSTIM1 re-expression reversed the effect of STIM1 knockdown on a number of migrating cells (*Figure 4D*). In addition, we evaluated the effect of siRNA targeted against rSTIM1 on SOCE, which was activated by the depletion of intracellular  $\text{Ca}^{2+}$  stores using  $1 \mu\text{M}$  TG in the absence of extracellular  $\text{Ca}^{2+}$ , followed by the addition of extracellular  $\text{Ca}^{2+}$  to 2 mM. The TG-mediated SOCE may be attributed to the release of  $\text{Ca}^{2+}$  from the SR. The infection of Ad-si/rSTIM1 (MOI 15 pfu/cell at 48 h after infection) resulted in a marked decrease in SOCE. However, the cotransfection of cells with Ad-hSTIM1 (MOI 15 pfu/cell) reversed the effect of STIM1 knockdown on intracellular  $\text{Ca}^{2+}$  of VSMCs (*Figure 4E*). These results demonstrated that SOCE influx may have a key role in VSMC proliferation.

### 3.5 The role of STIM1 in regulating the VSMC cell cycle

We used flow cytometry to examine the possible alteration of the cell cycle in response to STIM1 knockdown. Cultured VSMCs were first synchronized and stimulated with serum to initiate cell-cycle progression, and then infected with NSC, Ad-hSTIM1, and Ad-si/rSTIM1 for 48 h. Fluorescence-activated cell sorting was used to examine cell-cycle distribution (*Figure 5A*). Approximately 13% of VSMCs infected by NSC (MOI 30 pfu/cell) or 16% of uninfected VSMCs progressed into the S phase. VSMCs infected by Ad-si/rSTIM1 (MOI 30 pfu/cell) were distributed mainly in the G<sub>0</sub>/G<sub>1</sub> phase, and only 1.6% of cells progressed into the S phase. After VSMCs were transfected with Ad-hSTIM1 (MOI 15 pfu/cell), ~16% of cells progressed into the S phase (*Figure 5B*). The effect of STIM1 knockdown on cell-cycle arrest was also manifest by alterations in key components of the cell-cycle regulatory machinery. STIM1 knockdown caused an increase in the expression of the CDK inhibitor p21 and a significant reduction in the phosphorylation of Rb(pRb), thus permitting

the accumulation of the hypo-phosphorylated, growth-suppressive form of Rb (*Figure 5C*).

## 4. Discussion

The present results identify a critical role for STIM1 in neointimal formation in a rat model of vascular injury and suggest a potential role for STIM1 knockdown in the reduction of neointimal development. Meanwhile, we have demonstrated that STIM1 is a powerful regulator of cell proliferation both *in vivo* and *in vitro*. This conclusion is based on several independent lines of evidence. First, an overt upregulation of STIM1 expression *in vivo* was associated with balloon injury-induced VSMC hyper-proliferation in rat carotid arteries. Secondly, knockdown of endogenous STIM1 by adenoviral delivery of siRNA significantly suppressed neointimal hyperplasia *in vivo*, which was reversed by STIM1 replenishment. Thirdly, STIM1 knockdown inhibited SOCE in cultured VSMCs and blocked serum-induced VSMCs proliferation *in vitro*, which was also reversed by STIM1 replenishment. In addition, suppression of STIM1 also inhibits VSMCs migration *in vitro*. These observations suggest that expression and function of STIM1 after vascular injury may contribute to neointimal formation.

It is clear that increased  $\text{Ca}^{2+}$  influx is an important stimulus for SMC proliferation. Recently, it has been reported that transient receptor potential (TRP) channel genes encode  $\text{Ca}^{2+}$  channels that are responsible for  $\text{Ca}^{2+}$  entry during smooth muscle cell proliferation.<sup>10,23</sup> TRP was found first in *Drosophila* and has an essential role in the visual response of the fly.<sup>24</sup> Several homologues of the TRP channel family, such as TRPC1 and TRPC6, are expressed in mammalian cells and have intriguing sensing capabilities for a range of factors, including redox status and growth factors.<sup>23,25,26</sup> Yu *et al.*<sup>27</sup> reported that inhibition of TRPC6 expression with TRPC6 siRNA markedly attenuated the proliferation of pulmonary artery smooth muscle cells. Kumar *et al.*<sup>23</sup> reported that a specific E3-targeted antibody to TRPC1 and the chemical blocker 2-aminoethoxydiphenyl borate significantly reduced neointimal growth in human veins, as well as  $\text{Ca}^{2+}$  entry and proliferation of smooth muscle cells in culture. There is evidence that TRP channel genes encode subunits that form SOC channels in many cell types, including SMC.<sup>28,32</sup>  $\text{Ca}^{2+}$  entry through SOC increases intracellular  $\text{Ca}^{2+}$ , allowing for phosphorylation of signal transduction proteins and transcription factors, which are essential for the progression of the cell cycle.<sup>29,30</sup> Other major functions of the SOCE pathway are believed to be maintenance of SR  $\text{Ca}^{2+}$  levels, which are required for VSMC proliferation.<sup>31</sup> Activation of SOCE is triggered by a reduction in SR  $\text{Ca}^{2+}$  concentration. More recently, an RNAi-based screening approach revealed the novel membrane-spanning protein STIM1 to be required for the activation of SOC.<sup>12</sup> STIM1 is dispersed on the ER membrane in quiescence, and  $\text{Ca}^{2+}$  store depletion stimulates redistribution of STIM1 to the PM. The redistribution is thought to transmit a store depletion signal to the SOC in the PM.<sup>32</sup> In the present study, we demonstrated that direct inhibition of STIM1 can attenuate an SOC-mediated increase of intracellular  $\text{Ca}^{2+}$  and suppress VSMCs proliferation, which reduced neointimal development. Takahashi and Lu have reported that STIM1 knockdown can suppress VSMCs proliferation *in vitro*.<sup>33,34</sup> Spassova *et al.*<sup>14</sup> showed that re-expression of hSTIM1 in

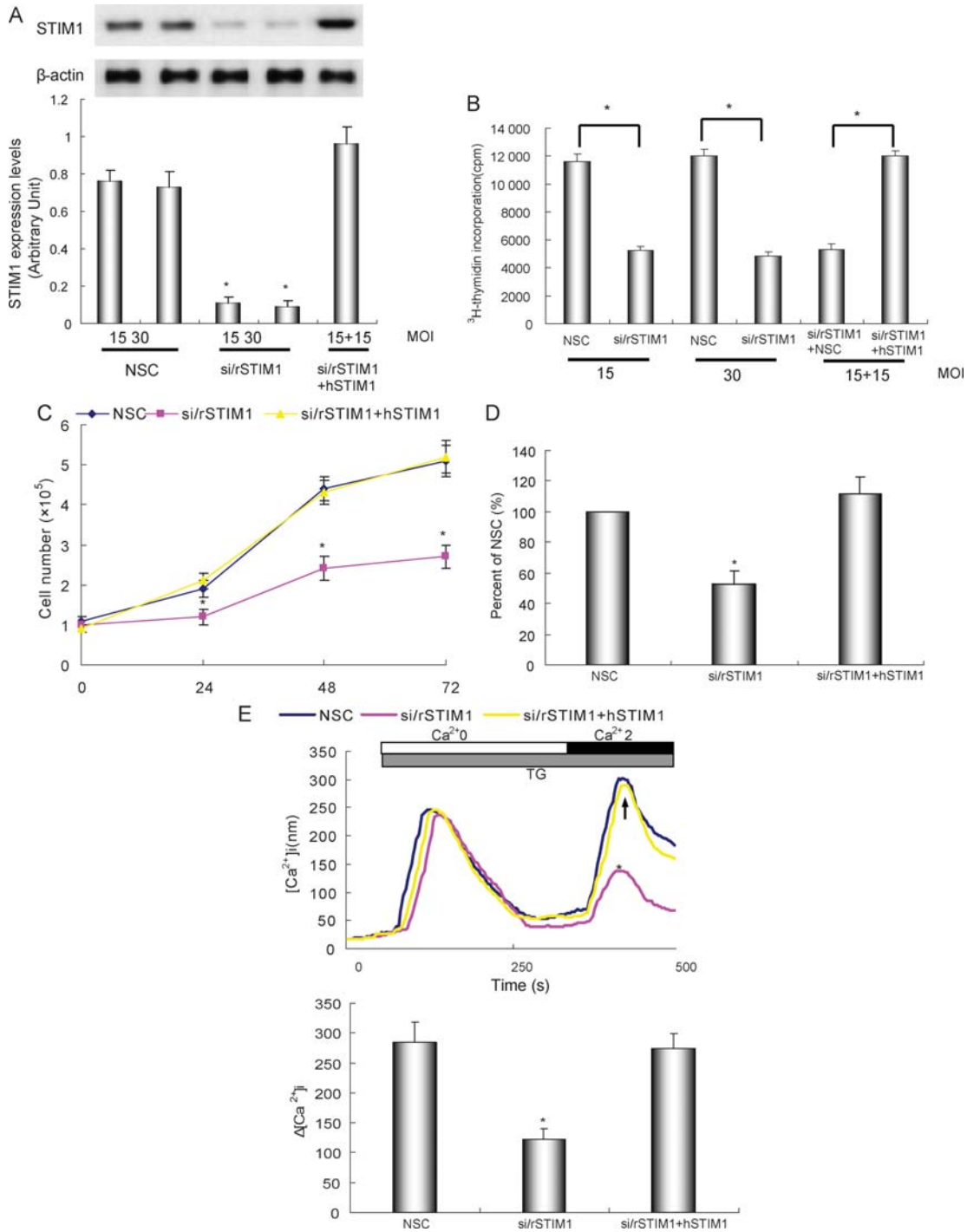


**Figure 4** (A) Top: The expression of stromal interaction molecule 1 protein was studied using western blotting. Transduction of vascular smooth muscle cells with increasing MOIs of Ad-si/rSTIM1 effectively decreased stromal interaction molecule 1 protein expression at 48 h post-transduction. When the transfection of Ad-hSTIM1 (MOI 15 pfu/cell) with Ad-si/rSTIM1 (MOI 15 pfu/cell) restored the expression of protein stromal interaction molecule 1. The data shown are representative of six different experiments. Bottom: Densitometric analysis of stromal interaction molecule 1 protein expression levels, normalized to expression levels of the housekeeping  $\beta$ -actin gene, was determined by Quantity One program. The results are expressed as mean  $\pm$  SEM of six experiments. \* $P < 0.05$  vs. non-silencing control and small interfering RNAs against rSTIM1 plus hSTIM1. (B) Transfection of vascular smooth muscle cells with Ad-si/rSTIM1 decreased the uptake of  $^3\text{H}$ thymidine by vascular smooth muscle cells significantly at 48 h after infection. In this rSTIM1 knockdown background, hSTIM1 re-expression reversed the effect of stromal interaction molecule 1 knockdown on  $^3\text{H}$ thymidine uptake. The data are presented as the mean  $\pm$  SEM ( $n = 12$ ). (C) Transfection of vascular smooth muscle cells with Ad-si/rSTIM1 suppressed the proliferation of vascular smooth muscle cells significantly at 48 h after infection (MOI 30 pfu/cell). hSTIM1 re-expression reversed the effect of stromal interaction molecule 1 knockdown on vascular smooth muscle cells proliferation. The data are presented as the mean  $\pm$  SEM ( $n = 3$ ). \* $P < 0.05$  vs. non-silencing control and si/rSTIM1+hSTIM1. (D) The cells of the non-silencing control group that migrated across the polycarbonate membrane were assigned a value of 100% and used to normalize the data for the other groups. The data are presented as the mean  $\pm$  SEM ( $n = 3$ ). \* $P < 0.05$  vs. non-silencing control and small interfering RNAs against rSTIM1 plus hSTIM1. (E) We measured the SOC-mediated influx of  $\text{Ca}^{2+}$  following stimulation with  $1 \mu\text{M}$  thapsigargin during the change from  $\text{Ca}^{2+}$ -free conditions to  $2 \text{ mM}$   $\text{Ca}^{2+}$ . Top: The infection of Ad-si/rSTIM1 (MOI 30 pfu/cell at 48 h after infection) resulted in a marked decrease in SOC. The cotransfection of cells with the recombinant hSTIM1 protein reversed the effect of stromal interaction molecule 1 knockdown on  $[\text{Ca}^{2+}]_i$  of vascular smooth muscle cells. Bottom: Statistical analysis of SOC in different groups. The data are presented as the mean  $\pm$  SEM ( $n = 6$ ). \* $P < 0.05$  vs. non-silencing control and si/rSTIM1 + hSTIM1.

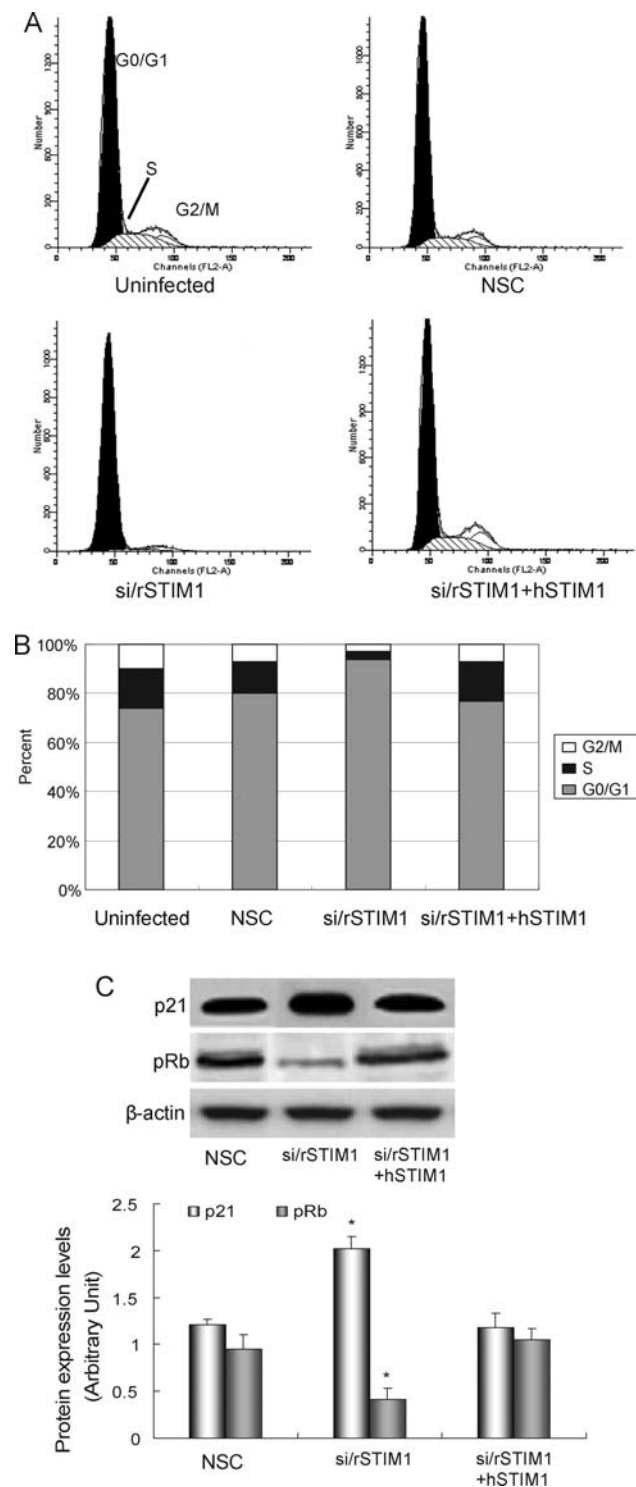


**Figure 5** (A) The alteration of the cell cycle in response to stromal interaction molecule 1 knockdown using flow cytometry. Typical examples of cell-cycle distribution in synchrony. (B) The average data of the cell-cycle distributions ( $n = 6$ ). (C) Stromal interaction molecule 1 knockdown caused an increase in the expression of p21 and a significant reduction in the phosphorylation of Rb in vascular smooth muscle cells. The data are presented as mean  $\pm$  SEM ( $n = 6$ ). \* $P < 0.05$  vs. non-silencing control and si/rSTIM1 + hSTIM1.

rat basophilic lymphoma cells of rSTIM1 knockdown could restore the activity of SOC. Our data indicated that re-expression of hSTIM1 in VSMCs reversed the effect of

STIM1 knockdown on intracellular  $Ca^{2+}$ , cell proliferation, and neointimal development.

In addition, we have demonstrated that STIM1 knockdown-induced suppression of VSMC proliferation is associated with an increase in the expression of the CDK inhibitor p21. Meanwhile, STIM1 knockdown attenuates phosphorylation of Rb, resulting in the accumulation of hypo-phosphorylated Rb in cultured VSMCs; Rb is one of the major modulators of the G1/S transition in mammalian cells. When hypo-phosphorylated in G0/G1, Rb blocks cell-cycle progression by binding to and suppressing the activities of transcription factors such as E2F family members.<sup>35,36</sup> Consistent with this, the increase in growth-suppressive, hypo-phosphorylated Rb contributes, at least in part, to STIM1 knockdown-induced cell-cycle arrest in G0/G1.

In summary, we show that STIM1 is a critical regulator of VSMC proliferation and neointimal hyperplasia. STIM1 may represent a novel therapeutic target in the prevention of restenosis after vascular intervention.

## Supplementary material

Supplementary Material is available at *Cardiovascular Research* online.

## Acknowledgement

We thank Yan-Yan Wang for excellent technical help.

**Conflict of interest:** none declared.

## Funding

This study was supported, in part, by a grant (no. 30700889) from the National Natural Science Foundation of China.

## References

- Glass CK, Witztum JL. Atherosclerosis. The road ahead. *Cell* 2001;104: 503–516.
- Levonon AL, Inkala M, Heikura T, Jauhainen S, Jyrkkänen HK, Kansanen E *et al.* Nrf2 gene transfer induces antioxidant enzymes and suppresses smooth muscle cell growth in vitro and reduces oxidative stress in rabbit aorta in vivo. *Arterioscler Thromb Vasc Biol* 2007;27:741–747.
- Magnier-Gaubil C, Herbert JM, Quarck R, Papp B, Corvazier E, Wuytack F *et al.* Smooth muscle cell cycle and proliferation. Relationship between calcium influx and sarco-endoplasmic reticulum  $Ca^{2+}$  ATPase regulation. *J Biol Chem* 1996;271:27788–27794.
- Munaron L, Antoniotti S, Fiorio Pla A, Lovisolo D. Blocking  $Ca^{2+}$  entry: a way to control cell proliferation. *Curr Med Chem* 2004;11:1533–1543.
- Quignard JF, Harricane MC, Menard C, Lory P, Nargeot J, Capron L *et al.* Transient down-regulation of L-type  $Ca^{2+}$  channel and dystrophin expression after balloon injury in rat aortic cells. *Cardiovasc Res* 2001; 49:177–188.
- Fellner SK, Arendshorst WJ. Store-operated  $Ca^{2+}$  entry is exaggerated in fresh preglomerular vascular smooth muscle cells of SHR. *Kidney Int* 2002;61:2132–2141.
- Park KM, Trucillo M, Serban N, Cohen RA, Bolotina VM. Role of iPLA2 and store-operated channels in agonist-induced  $Ca^{2+}$  influx and constriction in cerebral, mesenteric, and carotid arteries. *Am J Physiol Heart Circ Physiol* 2008;294:H1183–H1187.
- Weiss H, Amberger A, Widschwendter M, Margreiter R, Ofner D, Dietl P. Inhibition of store-operated calcium entry contributes to the anti-proliferative effect of non-steroidal anti-inflammatory drugs in human colon cancer cells. *Int J Cancer* 2001;92:877–882.
- Chiu WT, Tang MJ, Jao HC, Shen MR. Soft substrate up-regulates the interaction of STIM1 with store-operated  $Ca^{2+}$  channels that lead to normal epithelial cell apoptosis. *Mol Biol Cell* 2008;19:2220–2230.



10. Takahashi Y, Watanabe H, Murakami M, Ohba T, Radovanovic M, Ono K *et al.* Involvement of transient receptor potential canonical 1 (TRPC1) in angiotensin II-induced vascular smooth muscle cell hypertrophy. *Atherosclerosis* 2007;**195**:287–296.
11. Parekh AB. Store-operated  $\text{Ca}^{2+}$  entry: dynamic interplay between endoplasmic reticulum, mitochondria and plasma membrane. *J Physiol* 2003;**547**:333–348.
12. Roos J, DiGregorio PJ, Yeromin AV, Ohlsen K, Lioudyno M, Zhang S *et al.* STIM1, an essential and conserved component of store-operated  $\text{Ca}^{2+}$  channel function. *J Cell Biol* 2005;**169**:435–445.
13. Liou J, Kim ML, Heo WD, Jones JT, Myers JW, Ferrell JE Jr *et al.* STIM is a  $\text{Ca}^{2+}$  sensor essential for  $\text{Ca}^{2+}$ -store-depletion-triggered  $\text{Ca}^{2+}$  influx. *Curr Biol* 2005;**15**:1235–1241.
14. Spassova MA, Soboloff J, He LP, Xu W, Dziadek MA, Gill DL. STIM1 has a plasma membrane role in the activation of store-operated  $\text{Ca}^{2+}$  channels. *Proc Natl Acad Sci USA* 2006;**103**:4040–4045.
15. Clowes AW, Reidy MA, Clowes MM. Kinetics of cellular proliferation after arterial injury. I. Smooth muscle growth in the absence of endothelium. *Lab Invest* 1983;**49**:327–333.
16. Guo RW, Yang LX, Wang H, Liu B, Wang L. Angiotensin II induces matrix metalloproteinase-9 expression via a nuclear factor- $\kappa$ B-dependent pathway in vascular smooth muscle cells. *Regul Pept* 2008;**147**:37–44.
17. Chadjichristos CE, Matter CM, Roth I, Sutter E, Pelli G, Luscher TF *et al.* Reduced connexin43 expression limits neointima formation after balloon distension injury in hypercholesterolemic mice. *Circulation* 2006;**113**:2835–2843.
18. Kaplan-Albuquerque N, Van Putten V, Weiser-Evans MC, Nemenoff RA. Depletion of serum response factor by RNA interference mimics the mitogenic effects of platelet derived growth factor-BB in vascular smooth muscle cells. *Circ Res* 2005;**97**:427–433.
19. Chomczynski P, Sacchi N. Single step method of RNA isolation by acid guanidinium thiocyanate-phenol-chloroform extraction. *Anal Biochem* 1987;**162**:156–159.
20. Maffia P, Grassia G, Di Meglio P, Carnuccio R, Berrino L, Garside P *et al.* Neutralization of interleukin-18 inhibits neointimal formation in a rat model of vascular injury. *Circulation* 2006;**114**:430–437.
21. Murakami M, Xu F, Miyoshi I, Sato E, Ono K, Iijima T. Identification and characterization of the murine TRPM4 channel. *Biochem Biophys Res Commun* 2003;**307**:522–528.
22. Cao H, Dronadula N, Rizvi F, Li Q, Srivastava K, Gerthoffer WT *et al.* Novel role for STAT-5B in the regulation of Hsp27-FGF-2 axis facilitating thrombin-induced vascular smooth muscle cell growth and motility. *Circ Res* 2006;**98**:913–922.
23. Kumar B, Dreja K, Shah S, Cheong A, Xu SZ, Sukumar P *et al.* Upregulated TRPC1 channel in vascular injury in vivo and its role in human neointimal hyperplasia. *Circ Res* 2006;**98**:557–563.
24. Cosens DJ, Manning A. Abnormal electroretinogram from a *Drosophila* mutant. *Nature* 1969;**224**:285–287.
25. Fleming I, Rueben A, Popp R, Fisslthaler B, Schrodt S, Sander A *et al.* Epoxyeicosatrienoic acids regulate Trp channel dependent  $\text{Ca}^{2+}$  signaling and hyperpolarization in endothelial cells. *Arterioscler Thromb Vasc Biol* 2007;**27**:2612–2618.
26. Clapham DE. TRP channels as cellular sensors. *Nature* 2003;**426**:517–524.
27. Yu Y, Fantozzi I, Remillard CV, Landsberg JW, Kunichika N, Platoshyn O *et al.* Enhanced expression of transient receptor potential channels in idiopathic pulmonary arterial hypertension. *Proc Natl Acad Sci USA* 2004;**101**:13861–13866.
28. Xu SZ, Beech DJ. TrpC1 is a membrane-spanning subunit of store operated  $\text{Ca}^{2+}$  channels in native vascular smooth muscle cells. *Circ Res* 2001;**88**:84–87.
29. Pulver RA, Rose-Curtis P, Roe MW, Wellman GC, Lounsbury KM. Store-operated  $\text{Ca}^{2+}$  entry activates the CREB transcription factor in vascular smooth muscle. *Circ Res* 2004;**94**:1351–1358.
30. Pulver-Kaste RA, Barlow CA, Bond J, Watson A, Penar PL, Tranmer B *et al.*  $\text{Ca}^{2+}$  source-dependent transcription of CRE-containing genes vascular smooth muscle. *Am J Physiol Heart Circ Physiol* 2006;**291**:97–105.
31. Sweeney M, Yu Y, Platoshyn O, Zhang S, McDaniel SS, Yuan JX. Inhibition of endogenous TRP1 decreases capacitative  $\text{Ca}^{2+}$  entry and attenuates pulmonary artery smooth muscle cell proliferation. *Am J Physiol Lung Cell Mol Physiol* 2002;**283**:L144–L155.
32. Huang GN, Zeng W, Kim JY, Yuan JP, Han L, Muallem S *et al.* STIM1 carboxyl-terminus activates native SOC, I(crac) and TRPC1 channels. *Nat Cell Biol* 2006;**8**:1003–1010.
33. Takahashi Y, Watanabe H, Murakami M, Ono K, Munehisa Y, Koyama T *et al.* Functional role of stromal interaction molecule 1 (STIM1) in vascular smooth muscle cells. *Biochem Biophys Res Commun* 2007;**361**:934–940.
34. Lu W, Wang J, Shimoda LA, Sylvester JT. Differences in STIM1 and TRPC expression in proximal and distal pulmonary arterial smooth muscle are associated with differences in  $\text{Ca}^{2+}$  responses to hypoxia. *Am J Physiol Lung Cell Mol Physiol* 2008;**295**:L104–L113.
35. Harbour JW, Dean DC. Rb function in cell-cycle regulation and apoptosis. *Nature Cell Biol* 2000;**2**:E65–E67.
36. DeGregori J, Kowalik T, Nevins JR. Cellular targets for activation by the E2F1 transcription factor include DNA synthesis- and G1/S-regulatory genes. *Mol Cell Biol* 1995;**15**:4215–4224.